

Short Communication

Characterization and Electrochemical Properties of 10 mol% Lutetium-Doped BaCO₃ and its Composite Electrolyte for Intermediate Temperature Fuel Cells

De-Qian Huang^{1,3,*}, Yu-Jie Cao^{1,3}, Peng Sun^{1,2}, Nan Wang^{1,2}, Jing-Jing Zhu^{1,2}, Xiu-Ru Li^{1,3}, Ya-Ru Chen^{1,3}, Hai Wu^{1,3}, Hong Zhang^{1,3}, Liang-Quan Sheng^{1,3*}

¹ School of Chemistry and Material Engineering, Fuyang Normal University, Anhui, Fuyang, 236037, P. R. China

² Anhui Provincial Key Laboratory for Degradation and Monitoring of Pollution of The Environment, Fuyang Anhui 236037, P. R. China

³ Engineering Research Centre of Biomass Conversion and Pollution Prevention Control of Anhui Provincial Department of Education, Fuyang 236037, P. R. China

*E-mail: huangdeqian@163.com, Shenglq@fynu.edu.cn

Received: 12 February 2020 / Accepted: 7 April 2020 / Published: 10 May 2020

In this study, BaCe_{0.9}Lu_{0.1}O_{3-α} was prepared by a sol-gel method. Subsequently, it was combined with molten carbonates and chlorides to synthesize BaCe_{0.9}Lu_{0.1}O_{3-α}-(Na/K)Cl-(K/Li)₂CO₃ composite electrolyte. Structural characterizations and intermediate temperature electrochemical properties of BaCe_{0.9}Lu_{0.1}O_{3-α} and BaCe_{0.9}Lu_{0.1}O_{3-α}-(Na/K)Cl-(K/Li)₂CO₃ were investigated at 400–700 °C. X-ray diffraction showed that the main structure of BaCe_{0.9}Lu_{0.1}O_{3-α}-(Na/K)Cl-(K/Li)₂CO₃ was BaCeO₃ phase. The highest conductivity of BaCe_{0.9}Lu_{0.1}O_{3-α}-(Na/K)Cl-(K/Li)₂CO₃ was 6.8×10⁻² S·cm⁻¹ at 700 °C.

Keywords: Defects; Electrolytes; Fuel cell; Conductivity; Composite

1. INTRODUCTION

Solid oxide fuel cells (SOFCs), as an efficient and clean energy technology, have good application prospects [1–7]. The performances and applications of SOFCs are often determined by the dense electrolytes with ionic conductivities [8–13]. Iwahara et al. found that Ba(Sr)CeO₃-based oxides have excellent protonic conduction at high temperatures (600–1000 °C) [14]. Trivalent rare earth cation-doped BaCeO₃ has been widely studied [15–23]. For example, Guo et al. synthesized BaCe_{1-x}Y_xO_{3-α} by

a microemulsion method and studied the protonic conduction at 300–600 °C [20]. Because the ionic radius of Lu^{3+} is close to that of Ce^{4+} , investigation of Lu^{3+} -doped BaCeO_3 is particularly necessary.

Over the past 20 years, the designs of new oxygen ion-proton and oxygen ion-inorganic salt composite electrolyte materials have been widely studied [24–31]. Meng et al. synthesized $\text{Ce}_{0.9}\text{Gd}_{0.1}\text{O}_{1.95}$ - LiCl - SrCl_2 composite electrolyte [24]. Liu et al. studied intermediate-temperature SOFC performance of $\text{BaCe}_{0.7}\text{In}_{0.3}\text{O}_{3-\delta}$ - $\text{Gd}_{0.1}\text{Ce}_{0.9}\text{O}_{2-\delta}$ composite electrolyte [26]. Huang et al. investigated conductivity, morphology and SOFC performance of $\text{BaCe}_{0.7}\text{Zr}_{0.1}\text{Y}_{0.2}\text{O}_{3-\alpha}$ - $(\text{Na/Li})_2\text{CO}_3$ composite electrolyte [31]. Our previous reports studied Yb^{3+} -doped BaCeO_3 - $(\text{Na/K})\text{Cl}$ and $\text{BaCe}_{0.9}\text{Er}_{0.1}\text{O}_{3-\alpha}$ - K_2SO_4 - BaSO_4 composite electrolytes [32–33]. However, up to now, there has been no report about barium cerate-compound inorganic salts.

In this study, $\text{BaCe}_{0.9}\text{Lu}_{0.1}\text{O}_{3-\alpha}$ was synthesized via a sol-gel method. Then, it was combined with compound inorganic salts to prepare $\text{BaCe}_{0.9}\text{Lu}_{0.1}\text{O}_{3-\alpha}$ - $(\text{Na/K})\text{Cl}$ - $(\text{K/Li})_2\text{CO}_3$ composite electrolyte. Structural characterizations and intermediate temperature electrochemical properties of the samples were investigated.

2. EXPERIMENTAL

2.1. Materials Synthesis and Sintering

$\text{BaCe}_{0.9}\text{Lu}_{0.1}\text{O}_{3-\alpha}$ was prepared by a sol-gel method with Lu_2O_3 (0.9948 g), $\text{Ba}(\text{CH}_3\text{COO})_2$ (12.7711 g), $\text{Ce}(\text{NH}_4)_2(\text{NO}_3)_6$ (24.6699 g) and citric acid as raw materials. Firstly, Lu_2O_3 was added to a small amount of nitric acid and heated to 90 °C for dissolution. $\text{Ba}(\text{CH}_3\text{COO})_2$, $\text{Ce}(\text{NH}_4)_2(\text{NO}_3)_6$ and citric acid were successively added for heating and dissolving. The solution was heated until it was viscous and burnt to obtain the primary powder. The powder was sintered at 1250 °C and 1550 °C for 5 h, respectively, to obtain $\text{BaCe}_{0.9}\text{Lu}_{0.1}\text{O}_{3-\alpha}$. NaCl - KCl (1:1 mole ratio) and Li_2CO_3 - K_2CO_3 (68:32 mole ratio) were mixed and heated once to form a solid solution. The mixtures of $\text{BaCe}_{0.9}\text{Lu}_{0.1}\text{O}_{3-\alpha}$, NaCl - KCl and Li_2CO_3 - K_2CO_3 (weight ratio 7:2:1) were heated at 750 °C for 1 h to obtain $\text{BaCe}_{0.9}\text{Lu}_{0.1}\text{O}_{3-\alpha}$ - $(\text{Na/K})\text{Cl}$ - $(\text{K/Li})_2\text{CO}_3$ (BCLu - $(\text{Na/K})\text{Cl}$ - $(\text{K/Li})_2\text{CO}_3$) composite electrolyte.

2.2 Instrumentation

The structures of $\text{BaCe}_{0.9}\text{Lu}_{0.1}\text{O}_{3-\alpha}$ and $\text{BaCe}_{0.9}\text{Lu}_{0.1}\text{O}_{3-\alpha}$ - $(\text{Na/K})\text{Cl}$ - $(\text{K/Li})_2\text{CO}_3$ were measured by Raman spectrometer (iHR550) and X-ray diffraction (XRD, X-D-3, China). The morphologies of the samples were characterized by scanning electron microscope (SEM, Sigma 500). In order to test the AC impedances of the samples, Ag-Pd paste was coated on both sides of $\text{BaCe}_{0.9}\text{Lu}_{0.1}\text{O}_{3-\alpha}$ and $\text{BaCe}_{0.9}\text{Lu}_{0.1}\text{O}_{3-\alpha}$ - $(\text{Na/K})\text{Cl}$ - $(\text{K/Li})_2\text{CO}_3$. The thickness and area of the samples were 1.0 mm and 0.5 cm^2 , respectively. The test temperature range was 400–700 °C with a CHI660E electrochemical analyzer (Chenhua, Shanghai). The relationship between conductivity and $p\text{O}_2$ was measured at 700 °C with different proportions of dry nitrogen, oxygen and hydrogen.

3. RESULTS AND DISCUSSION

3.1 Characterization of $\text{BaCe}_{0.9}\text{Lu}_{0.1}\text{O}_{3-\alpha}$ and $\text{BaCe}_{0.9}\text{Lu}_{0.1}\text{O}_{3-\alpha}(\text{Na/K})\text{Cl}(\text{K/Li})_2\text{CO}_3$.

Fig. 1 shows the Raman spectra of $\text{BaCe}_{0.9}\text{Lu}_{0.1}\text{O}_{3-\alpha}$ and $\text{BaCe}_{0.9}\text{Lu}_{0.1}\text{O}_{3-\alpha}(\text{Na/K})\text{Cl}(\text{K/Li})_2\text{CO}_3$. The vibration peak displayed at 130 cm^{-1} may be attributed to the stretching mode of the carbonate ion [23]. The vibrations near $310\text{--}360\text{ cm}^{-1}$ belong to the halide vibration and the characteristic peak is 358 cm^{-1} . The bands at 471 cm^{-1} and 673 cm^{-1} belong to the Ce-O F_{2g} mode and O_h vibrational mode, respectively [34]. The results show that $\text{BaCe}_{0.9}\text{Lu}_{0.1}\text{O}_{3-\alpha}(\text{Na/K})\text{Cl}(\text{K/Li})_2\text{CO}_3$ contains barium cerate, carbonate and chloride groups.

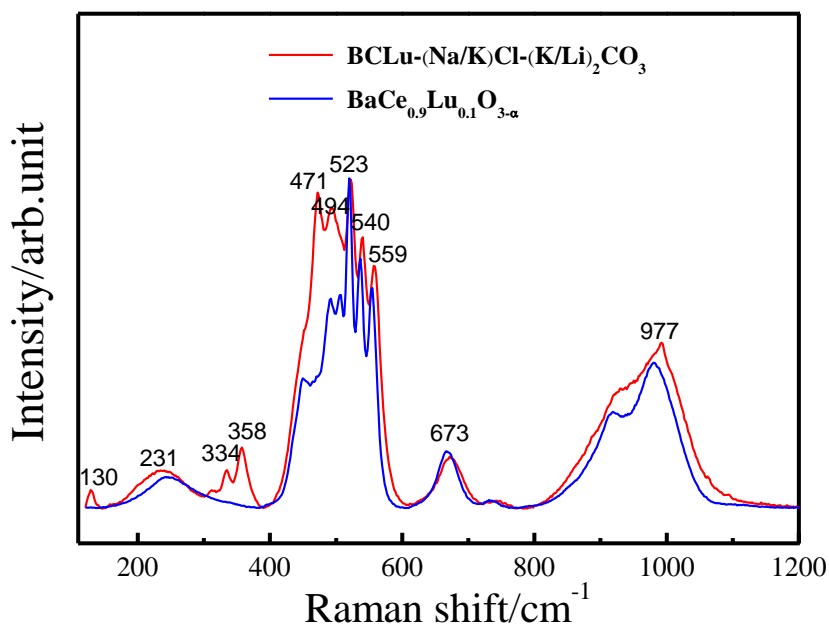


Figure 1. Raman spectra of $\text{BaCe}_{0.9}\text{Lu}_{0.1}\text{O}_{3-\alpha}$ and $\text{BaCe}_{0.9}\text{Lu}_{0.1}\text{O}_{3-\alpha}(\text{Na/K})\text{Cl}(\text{K/Li})_2\text{CO}_3$ (BCLu-(Na/K)Cl(K/Li) $_2$ CO $_3$).

Fig. 2 shows XRD patterns of $\text{BaCe}_{0.9}\text{Lu}_{0.1}\text{O}_{3-\alpha}$ and $\text{BaCe}_{0.9}\text{Lu}_{0.1}\text{O}_{3-\alpha}(\text{Na/K})\text{Cl}(\text{K/Li})_2\text{CO}_3$. The diffraction peaks of $\text{BaCe}_{0.9}\text{Lu}_{0.1}\text{O}_{3-\alpha}$ agree with Han and Guo et al. [15, 20]. For $\text{BaCe}_{0.9}\text{Lu}_{0.1}\text{O}_{3-\alpha}(\text{Na/K})\text{Cl}(\text{K/Li})_2\text{CO}_3$, the extra peaks are obvious and come from crystalline KCl, $(\text{Li-K})_2\text{CO}_3$ and NaCl respectively [28–29, 32]. Combined with the results of Fig. 1, there is no reaction between $\text{BaCe}_{0.9}\text{Lu}_{0.1}\text{O}_{3-\alpha}$ and $(\text{Na/K})\text{Cl}(\text{K/Li})_2\text{CO}_3$ after being heated at $750\text{ }^\circ\text{C}$.

The external and cross-sectional SEM diagrams of $\text{BaCe}_{0.9}\text{Lu}_{0.1}\text{O}_{3-\alpha}$ and $\text{BaCe}_{0.9}\text{Lu}_{0.1}\text{O}_{3-\alpha}(\text{Na/K})\text{Cl}(\text{K/Li})_2\text{CO}_3$ are shown in Fig. 3. It can be seen from Fig. 3(a, b) that the grains of $\text{BaCe}_{0.9}\text{Lu}_{0.1}\text{O}_{3-\alpha}$ are not fully fused. It can be considered that the sintering temperature ($1550\text{ }^\circ\text{C}$) did not reach the temperature for fully forming the grain boundary. There are very few non-penetrating holes in Fig. 3(b). Fig. 3(c, d) show that the molten chlorides and carbonates fill the holes between $\text{BaCe}_{0.9}\text{Lu}_{0.1}\text{O}_{3-\alpha}$ particles, therefore, densifying the composite after the process of heating [28–31].

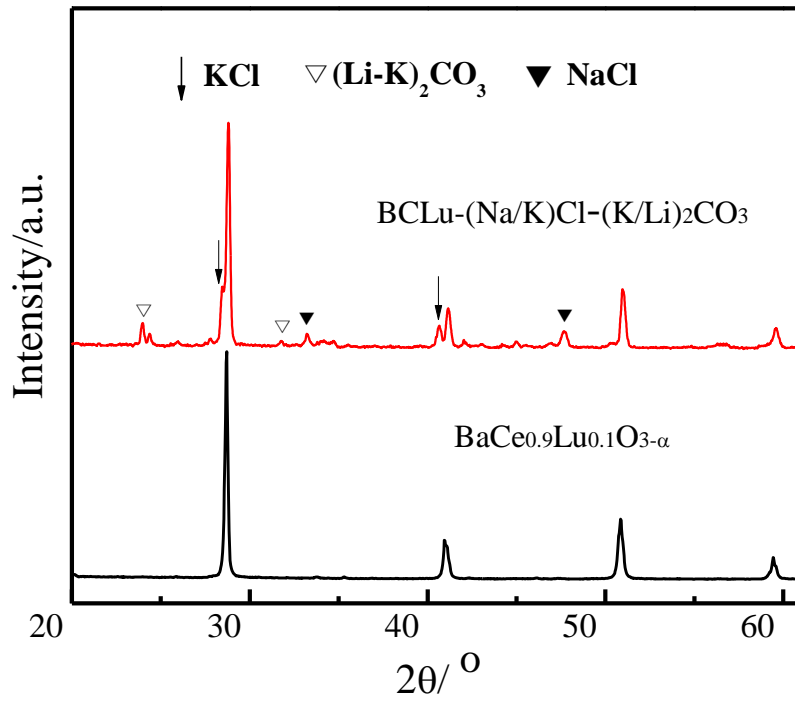


Figure 2. XRD diagrams of $\text{BaCe}_{0.9}\text{Lu}_{0.1}\text{O}_{3-\alpha}$ and $\text{BaCe}_{0.9}\text{Lu}_{0.1}\text{O}_{3-\alpha}-(\text{Na/K})\text{Cl}-(\text{K/Li})_2\text{CO}_3$ (BCLu-(Na/K)Cl-(K/Li) $_2$ CO $_3$).

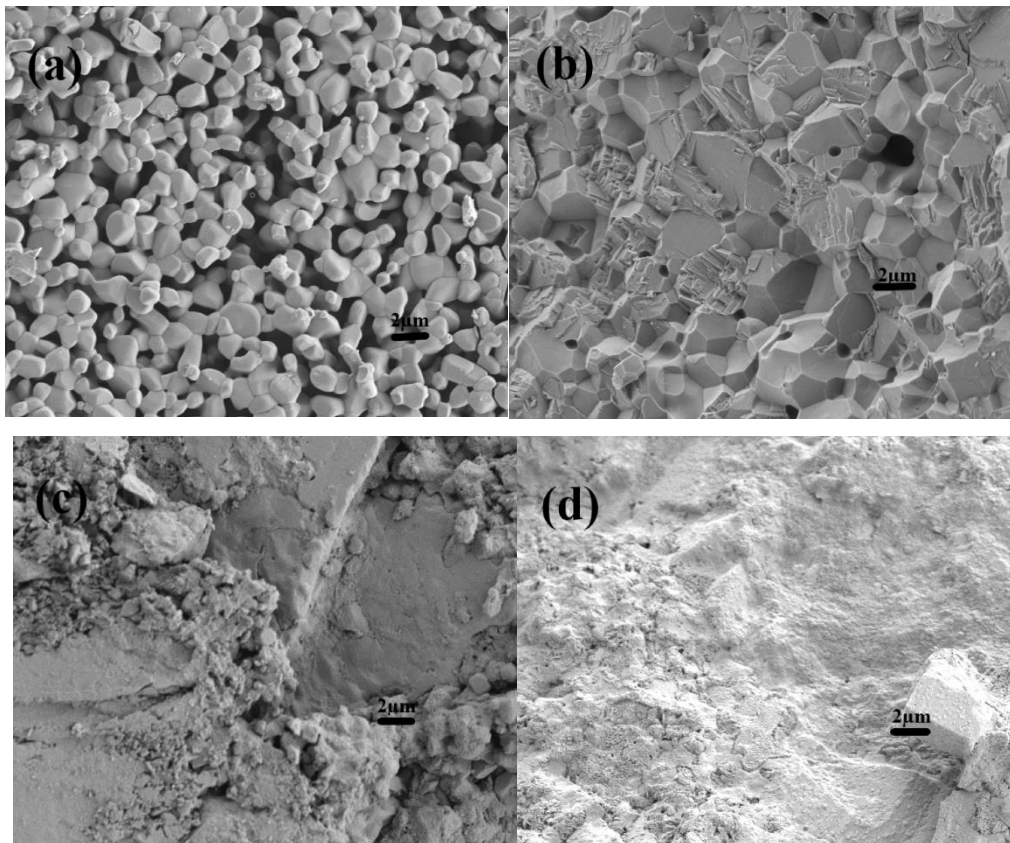


Figure 3. The external and cross-sectional SEM diagrams of $\text{BaCe}_{0.9}\text{Lu}_{0.1}\text{O}_{3-\alpha}$ (a,b) and $\text{BaCe}_{0.9}\text{Lu}_{0.1}\text{O}_{3-\alpha}-(\text{Na/K})\text{Cl}-(\text{K/Li})_2\text{CO}_3$ (c,d).

3.2 Conductivity of $\text{BaCe}_{0.9}\text{Lu}_{0.1}\text{O}_{3-\alpha}$ and $\text{BaCe}_{0.9}\text{Lu}_{0.1}\text{O}_{3-\alpha}(\text{Na/K})\text{Cl}(\text{K/Li})_2\text{CO}_3$

Fig. 4 shows the $\log(\sigma T) \sim 1000 T^{-1}$ plots of $\text{BaCe}_{0.9}\text{Lu}_{0.1}\text{O}_{3-\alpha}$ and $\text{BaCe}_{0.9}\text{Lu}_{0.1}\text{O}_{3-\alpha}(\text{Na/K})\text{Cl}(\text{K/Li})_2\text{CO}_3$ from 400 °C to 700 °C. From Fig. 4, it can be seen that the horizontal and vertical coordinates of the curves are basically linear. The conductivity of $\text{BaCe}_{0.9}\text{Lu}_{0.1}\text{O}_{3-\alpha}$ reaches the maximum value of $9.5 \times 10^{-3} \text{ S} \cdot \text{cm}^{-1}$ at 700 °C. Gui et al. reported that the conductivity of $\text{BaZr}_{0.3}\text{Ce}_{0.5}\text{Y}_{0.2}\text{O}_{3-\delta}$ supplemented with 2 mol% Bi_2O_3 was $1.04 \times 10^{-2} \text{ S} \cdot \text{cm}^{-1}$ at 700 °C [35]. The results show that the conductivity of $\text{BaCe}_{0.9}\text{Lu}_{0.1}\text{O}_{3-\alpha}$ is equivalent to the value reported in the literature. The conductivities of $\text{BaCe}_{0.9}\text{Lu}_{0.1}\text{O}_{3-\alpha}(\text{Na/K})\text{Cl}(\text{K/Li})_2\text{CO}_3$ are higher than that of $\text{BaCe}_{0.9}\text{Lu}_{0.1}\text{O}_{3-\alpha}$ in the temperature range of 400–700 °C. The maximum conductivity of $\text{BaCe}_{0.9}\text{Lu}_{0.1}\text{O}_{3-\alpha}(\text{Na/K})\text{Cl}(\text{K/Li})_2\text{CO}_3$ is $6.8 \times 10^{-2} \text{ S} \cdot \text{cm}^{-1}$ at 700 °C. It can be considered that molten inorganic salts can further promote the long range orderly ability of conducting ions between the interface and the bulk phase of $\text{BaCe}_{0.9}\text{Lu}_{0.1}\text{O}_{3-\alpha}(\text{Na/K})\text{Cl}(\text{K/Li})_2\text{CO}_3$ [25].

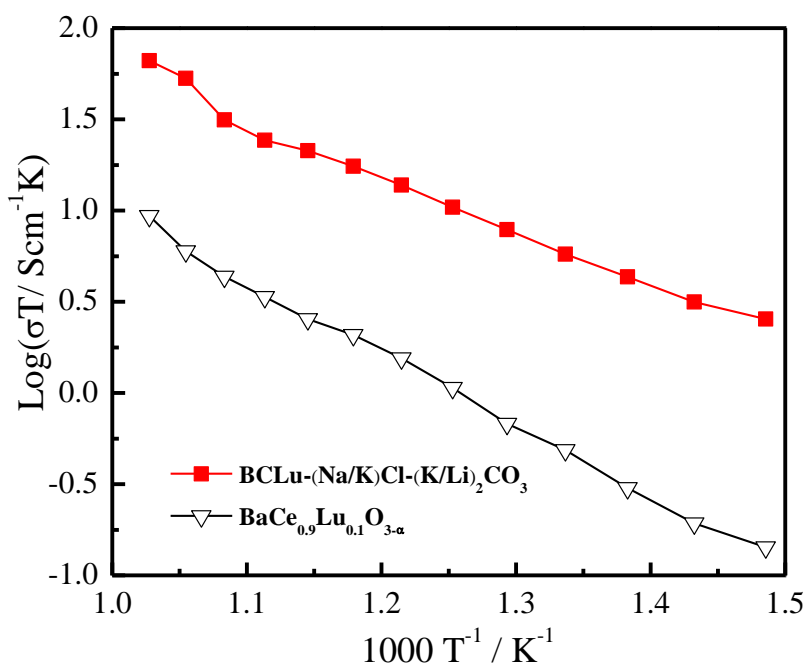


Figure 4. $\log(\sigma T) \sim 1000 T^{-1}$ plots of $\text{BaCe}_{0.9}\text{Lu}_{0.1}\text{O}_{3-\alpha}$ and $\text{BaCe}_{0.9}\text{Lu}_{0.1}\text{O}_{3-\alpha}(\text{Na/K})\text{Cl}(\text{K/Li})_2\text{CO}_3$ (BCLu-(Na/K)Cl-(K/Li)₂CO₃) at 400–700 °C.

Fig. 5 shows the relationship between conductivity and $p\text{O}_2$ of $\text{BaCe}_{0.9}\text{Lu}_{0.1}\text{O}_{3-\alpha}$ and $\text{BaCe}_{0.9}\text{Lu}_{0.1}\text{O}_{3-\alpha}(\text{Na/K})\text{Cl}(\text{K/Li})_2\text{CO}_3$ at 700 °C. The relationship between conductivity and $p\text{O}_2$ is usually measured to study the sample's ionic conduction. Lyagaeva et al. found that $\text{BaCe}_{0.5}\text{Zr}_{0.3}\text{Y}_{0.2-x}\text{Yb}_x\text{O}_{3-\alpha}$ was a pure ionic conductor at 600 °C [18]. In Fig. 5, the conductivities in nitrogen, oxygen and hydrogen under different $p\text{O}_2$ are almost the same, which shows that $\text{BaCe}_{0.9}\text{Lu}_{0.1}\text{O}_{3-\alpha}$ and $\text{BaCe}_{0.9}\text{Lu}_{0.1}\text{O}_{3-\alpha}(\text{Na/K})\text{Cl}(\text{K/Li})_2\text{CO}_3$ show ionic conduction at 700 °C.

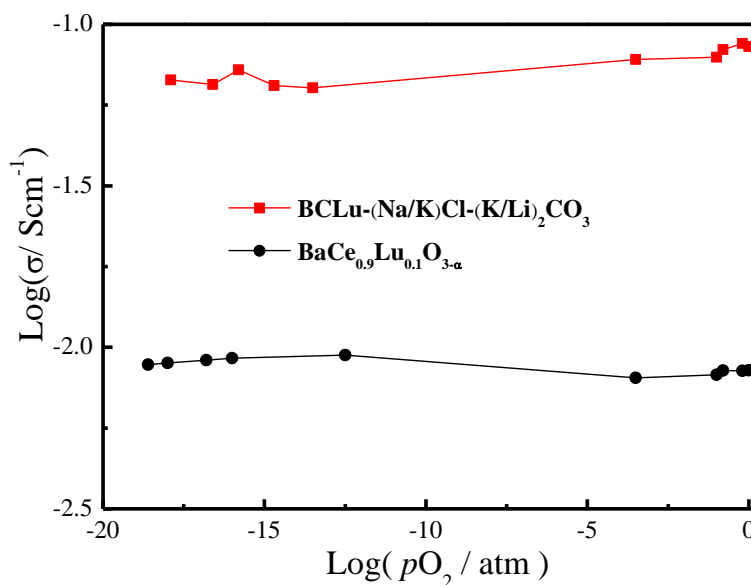


Figure 5. The $\log \sigma \sim \log (pO_2)$ plots of $BaCe_{0.9}Lu_{0.1}O_{3-\alpha}$ and $BaCe_{0.9}Lu_{0.1}O_{3-\alpha}-(Na/K)Cl-(K/Li)_2CO_3$ (BCLu-(Na/K)Cl-(K/Li) $_2$ CO $_3$) at 700 °C.

4. CONCLUSIONS

In this study, molten carbonates and chlorides were combined with $BaCe_{0.9}Lu_{0.1}O_{3-\alpha}$ to synthesize a new composite electrolyte, $BaCe_{0.9}Lu_{0.1}O_{3-\alpha}-(Na/K)Cl-(K/Li)_2CO_3$. The Raman spectrometer results showed that $BaCe_{0.9}Lu_{0.1}O_{3-\alpha}-(Na/K)Cl-(K/Li)_2CO_3$ contained barium cerate, carbonate and chloride groups. The SEM diagrams showed that the molten chlorides and carbonates filled and densified the composite. The relationship between conductivity and pO_2 showed that $BaCe_{0.9}Lu_{0.1}O_{3-\alpha}$ and $BaCe_{0.9}Lu_{0.1}O_{3-\alpha}-(Na/K)Cl-(K/Li)_2CO_3$ were ionic conductors at 700 °C.

ACKNOWLEDGEMENTS

This work is supported by Fuyang Municipal Government - Fuyang Normal College Horizontal Cooperation Major Project (XDHX201701) and Key Project (XDHX2016009), Innovation Team of Modern Analytical Technologies (kytd201701), Innovation and Entrepreneurship Program for college students of Anhui Province (S201910371028), and State Key Laboratory of Analytical Chemistry for Life Science (SKLACLS1712).

CONFLICTS OF INTEREST

None

References

1. L. Bi, S.P. Shafi, E.H. Da'as and E. Traversa, *Small*, 14 (2018) 1801231.
2. C. Bernuy-Lopez, L. Rioja-Monllor, T. Nakamura, S. Ricote, R. O'Hayre, K. Amezawa, M. Einarsrud and T. Grande, *Materials*, 11 (2018) 196.
3. Y.P. Xia, Z.Z. Jin, H.Q. Wang, Z.Gong, H.L. Lv, R.R. Peng, W. Liu and L. Bi, *J. Mater. Chem. A*, 7 (2019) 16136.
4. Y. Tian, Z. Lü, X. Guo and P. Wu, *Int. J. Electrochem. Sci.*, 14 (2019) 1093.

5. X. Xu, L. Bi and X.S. Zhao, *J. Membrane Sci.*, 558 (2018) 17.
6. A.A. Solovyev, S.V. Rabotkin, A.V. Shipilova and I.V. Ionov, *Int. J. Electrochem. Sci.*, 14 (2019) 575.
7. X. Xu, H.Q. Wang, J.M. Ma, W.Y. Liu, X.F. Wang, M. Fronzi and L. Bi, *J. Mater. Chem. A*, 7 (2019) 18792.
8. H. Jiang and F. Zhang, *Int. J. Electrochem. Sci.*, 15 (2020) 959.
9. J.M. Ma, Z.T. Tao, H.N. Kou, M. Fronzi and L. Bi, *Ceram. Int.*, 46 (2020) 4000.
10. H. Dai, H. Kou, Z. Tao, K. Liu, M. Xue, Q. Zhang and L. Bi, *Ceram. Int.*, 46 (2020) 6987.
11. E. H. Da'as, L. Bi, S. Boulfrad and E. Traversa, *Sci. China Mater.*, 61 (2018) 57.
12. J.-W. Ju, D.-M. Huan, Y.-X. Zhang, C.-R. Xia and G.-L. Cui, *Rare Met.*, 37 (2018) 734.
13. Y. N. Chen, T. Tian, Z. H. Wan, F. Wu, J. T. Tan and M. Pan, *Int. J. Electrochem. Sci.*, 13 (2018) 3827.
14. H. Iwahara, T. Esaka, H. Uchida and N. Maeda, *Solid State Ionics*, 3/4 (1981) 359.
15. Y. Han, R. Du, C. Wang, H. Zhai, F. Wu and H. Wang, *Int. J. Electrochem. Sci.*, 14 (2019) 7695.
16. N. Danilov, E. Pikalova, J. Lyagaeva, B. Antonov, D. Medvedev, A. Demin and P. Tsiakaras, *J. Power Sources*, 366 (2017) 161.
17. J. Xiao, L. Chen, H. Yuan, L. Ji, C. Xiong, J. Ma and X. Zhu, *Mater. Lett.*, 189 (2017) 192.
18. J. Lyagaeva, G. Vdovin, L. Hakimova, D. Medvedev, A. Demin and P. Tsiakaras, *Electrochim. Acta*, 251 (2017) 554.
19. G. S. Reddy and R. Bauri, *J. Alloy Compd.*, 688 (2016) 1039.
20. Y. Guo, B. Liu, Q. Yang, C. Chen, W. Wang and G. Ma, *Electrochem. Commun.*, 11 (2009) 153.
21. J.M. Sailaja, K.V. Babu, N. Murali and V. Veeraiah, *J. Adv. Res.*, 8 (2017) 169.
22. J. Song, B. Meng and X. Tan, *Ceram. Int.*, 42 (2016) 13278.
23. J.M. Sailaja, N. Murali, S.J. Margarete, T.W. Mammo and V. Veeraiah, *Results Phys.*, 8 (2018) 128.
24. Q. X. Fu, S. W. Zha, W. Zhang, D. K. Peng, G. Y. Meng and B. Zhu. Intermediate temperature fuel cells based on doped Ceria-LiCl-SrCl₂ composite electrolyte. *J. Power Sources*, 104 (2002) 73–78.
25. B. Zhu, S. Li and B.E. Mellander, *Electrochem. Commun.*, 10 (2008) 302.
26. F. Liu, J. Dang, J. Hou, J. Qian, Z. Zhu, Z. Wang and W. Liu, *J. Alloy Compd.*, 639 (2015) 252.
27. A.I.B. Rondao, S.G. Patricio, F.M.L. Figueiredo and F.M.B. Marques, *Int. J. Hydrogen Energy*, 39 (2014) 5460.
28. N.C.T. Martins, S. Rajesh and F.M.B. Marques, *Mater. Res. Bull.*, 70 (2015) 449.
29. K.-Y. Park, T.-H. Lee, J.-T. Kim, N. Lee, Y. Seo, S.-J. Song and J.-Y. Park, *J. Alloy Compd.*, 585 (2014) 103.
30. K.-Y. Park, T.-H. Lee, S. Jo, J. Yang, S.-J. Song, H.-T. Lim, J.H. Kim and J.-Y. Park, *J. Power Sources*, 336 (2016) 437.
31. Y. Hei, J. Huang, C. Wang and Z. Mao, *Int. J. Hydrogen Energy*, 39 (2014) 14328.
32. X. Jiang, F. Wu and H. Wang, *Materials*, 12 (2019) 739.
33. F. Wu, R. Du, T. Hu, H. Zhai and H. Wang, *Materials*, 12 (2019) 2752.
34. Y. Hou, J. Wu and E.Y. Konyshva, *Int. J. Hydrogen Energy*, 41(2016) 3994.
35. L. Gu, Y. Ling, G. Li, Z. Wang, Y. Wan, R. Wang, B. He and L. Zhao, *J. Power Sources*, 301(2016) 369.